iJournals: International Journal of Software & Hardware Research in Engineering
ISSN:2347-4890, ijournals.in/ijshre
Volume 12 Issue 5, May 2024

Implementation Of DGS And EVS in Distribution Networks for System Performance Enhancement

Authors: Mrityunjay Kumar Maurya; Imran Khan; Malik Rafi
AZAD Institute of Engineering & Technology, Lucknow
*****RR Institute of Engineering & Technology, Lucknow**
adarshhpl1995@gmail.com *, pe.imran@gmail.com, mali_rafi@rediffmail.com**

Abstract

The increase in plug-in electric vehicles (PEVs) is likely to see a noteworthy impact on the distribution system due to high electric power consumption during charging and uncertainty in charging behavior. To address this problem, the present work mainly focuses on optimal integration of distributed generators (DG) into radial distribution systems in the presence of PEV loads with their charging behavior under daily load pattern including load models by considering the daily (24 h) power loss and voltage improvement of the system as objectives for better system performance. Design/methodology/approach: To achieve the desired outcomes, an efficient weighted factor multi-objective function is modeled. Particle Swarm Optimization (PSO) and Butterfly Optimization (BO) algorithms are selected and implemented to minimize the objectives of the system. A repetitive backward-forward sweep-based load flow has been introduced to calculate the daily power loss and bus voltages of the radial distribution system. The simulations are carried out using MATLAB software. Findings: The simulation outcomes reveal that the proposed approach definitely improved the system performance in all aspects. Among PSO and BO, BO is comparatively successful in achieving the desired objectives. Originality/value: The main contribution of this paper is the formulation of the multi-objective function that can address daily active power loss and voltage deviation under 24-h load pattern including grouping of residential, industrial and commercial loads. Introduction of repetitive backward-forward sweep-based load flow and the modeling of PEV load with two different charging scenarios.

Key words: PEV, PV, PSO, GWO

1. Introduction

It is vital to use renewable energy as a fossil fuel substitute due to the extreme exploitation of outdated fossil fuels, which has led to more serious ecological pollution issues like energy resource scarcity and climate change, as the energy industry has developed sustainably [1]. The energy crisis has been lessened in recent years by the extensive adoption of renewable energy causes and new energy technology, but these developments have also presented difficult problems for control system optimization formation and subordinate energy rational operation. For example, in addition to problems with harmonic pollution, three-phase voltage imbalance, and transformer aging, the time-space dimensional decentralization of EV charging and the random and intermittent nature of power generated by WTs or PVs create more uncertainty than ever before for current DN operations [5–3]. Specifically, the extended PVD of the load curve increases the power system demands. It is commonly acknowledged that two crucial measures of the operational state of the DN are safety and economy, which are expressed as node voltage excursion and active power loss, respectively [9].

Due to the significant peak load caused by all of the EV users' combined charging habits, low voltage or even blackout is likely to occur, which also increases system loss. Guiding principles for coordinated regulation should be put into place in order to meet consumer needs for electricity and transportation while avoiding the negative consequences of integrated renewable energy and EVs. The Chinese government has recently heavily sponsored the IES and turned it into a research hotspot for two key reasons: the integration of renewable energy and the coordinated development of the multi-energy system. In light of the IES, the supply-oriented management idea has been superseded by the demand-oriented management concept for the DN, which combines the elements of distributed generation control, real-time monitoring, information sharing, and market transactions. Better scheduling and accommodations are made possible by this, allowing distributed energy equipment to be more diverse.

The BESS is now an essential supporting component to increase the compatibility near for the PV and WT of the DN in order to stabilize the output volatility of renewable control generation. Through electrochemical charging and discharging, the BESS transfers electricity, increasing the use of renewable vigorbases and their economic benefits

for the local grid while also enhancing power supply stability. To lessen high fluctuations connected to DG outputs, a hierarchical coordinated control method based on the MPC framework has been developed utilizing the fast-response BESS [6]. Furthermore, when incorporated into a vehicle-to-grid (V2G) system, EVs can also be seen as controllable power resources to provide bidirectional power flow between the building cluster and DN.

33-BUS TEST SYSTEM

Information about the updated 33-bus test system depicted in Fig. 1 is contained in this document. The following traits define the modified 33-bus test system, which is an adaption of the IEEE 33-bus test system:

The substation comprises seven zones and has a nominal voltage of 13.8 kV. Its substation transformer at bus 1 has a capacity of 3 MW.

• The loading factors for the three time segments under consideration are 80%, 60%, and 100% of the nominal value, respectively. The nominal demand for each bus is displayed in Table I.

• Tables II and III, respectively, contain data for the new and current distribution branches002E

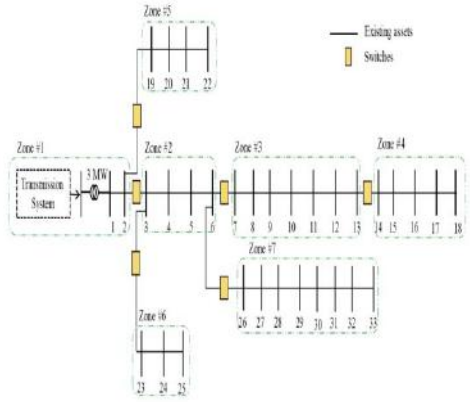

Figure 1. Illustrative 33-bus test system.

2. Particle Swarm Optimization:

PSO is a computational optimization method that draws inspiration from the social dynamics of natural systems, such as fish schools and bird flocks. It was developed as an optimization technique to find the optimal response within a search space.

Here's a brief rundown of how PSO functions:

Initialization: To begin, the algorithm generates a population of particles, or possible solutions. Any particle in the search space represents a likely solution.

Objective Function: A function that must be minimized or maximized defines the optimization challenge.

Movement and Update: Based on its own involvement (personal best) and the communal experience of the swarm (global best), each particle moves through the search space by modifying its position. Particles travel in an iterative manner, guided by velocity vectors that change their positions.

Evaluation: Using the objective function as a basis, each particle's fitness is assessed.

Update Personal and Global Bests: A particle updates its personal best if it finds a solution that is better than its previous best. In the same way, if the worldwide best solution

Termination: Until a finish condition is content, such as attainment a maximum number of repetitions or arriving at a workable solution, the algorithm iterates through these phases.

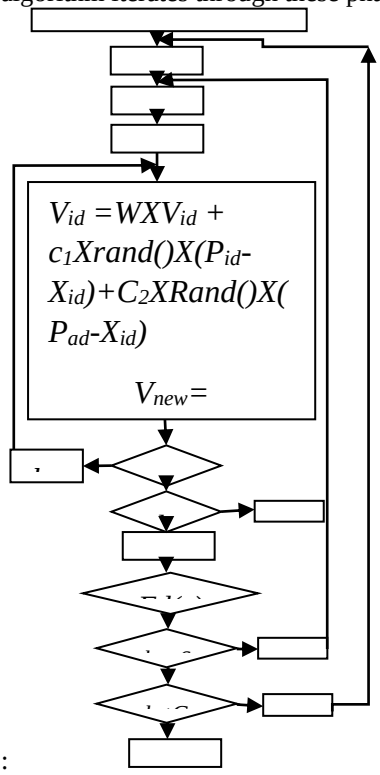

:

Figure 2. Flowchart of PSO

PSO is renowned for its ease of use and potency in effectively searching and utilizing the search field. It has been used in a variety of optimization scenarios, such as neural network training, engineering design, and other fields where identifying the best solution is essential.

3. Grey Wolf Optimization Algorithm

Metaheuristic optimization procedures are getting familiar in requests based on engineering due to easy concepts, simple implements that do not require large amount of system information. The modern optimization schemes are capable to bypass local optima and commonly used in a extensive range under dissimilar disciplines. Many procedures are present that are based on multiple combinative optimization difficulties. GWO is new approach [31] introduced in 2016. It is enthused by the grey wolf's social conduct that

working in leadership hierarchy for strategy to perform in hunting. Grey wolves are the top-level marauders; living in group of 5 to 15 wolves. The strategy of hunting classified into four groups α, β, Δ, and Ω. α-wolves taken as leader of the group that has authority of making decision for hunting place, asleep place and so on. α-wolves are leading and instruct others to follow them. They perform a main role to produce new solutions. β-wolves comes to next level they assistant α-wolves in decision-making. They take decision when alpha wolves are approved away. They listen to the α-wolves decision and deliveranswer to the α-wolves. The Δ-wolves are called subordinate wolves. They belong to elders, hunters, sentinels, caretakers and scouts. Δ-wolves follow alphas and betas and manage Ω-wolves. Ω-wolves are in lowest rank and play the role of scapegoat. They follow all other leading wolves. They are not significanthelp others from oppositeinteriorglitches.

Three types of hunting are distinguished in GWO: tracking, encircling, and assaulting the prey during the exploration and exploitation phase. Exploitation is the process of finding the best solution while encircling and attacking the prey, while tracking is the process of locating the best solution throughout a global search space.

When encircling, the prey's location is identified. During this stage, the prey's position vector is established, and searchers modify its location by determining the optimal solution to the equation below:

$$\vec{D} = \left[\vec{C}.\overrightarrow{X_P}(k) - \vec{X}(k)\right]$$
$$\vec{X}(k+1) = \overrightarrow{X_P}(k) - \vec{A}.\overrightarrow{D},$$

k: current iteration, $\vec{A}$ and $\vec{C}$: constant vectors, location vector of the prey, $\vec{X}$: position vector, | | : complete value, and '·' : element-by-element reproduction. The vectors $\vec{A}$ and $\vec{C}$ are:

$$\vec{A} = 2\vec{a}.\vec{r} - \vec{a}$$
$$\vec{C} = 2.\vec{r},$$

$\vec{a}$: reductions linearly from 2 to 0 and $\vec{r}$: accidental value in [0, 1]. The location of the search agent [X, Y] is accustomed based on the site of the prey gained so far [X^*, Y^*]. $\vec{A}$ and $\vec{C}$ attuned for achieving best agent in dissimilar places.

In hunting phase, α-wolves direct other wolves. Initially, α-wolve is first best answer, β-wolves: second-best answer and Δ-wolves is the third best solution. These three solutions are used to update the location of the lowest position solution omega. The hunting approachcalculation is given below:

$$\overrightarrow{D_\alpha} = \left|\overrightarrow{C_1} * \overrightarrow{X_\alpha} - \vec{X}\right|$$
$$\overrightarrow{D_\beta} = \left|\overrightarrow{C_2} * \overrightarrow{X_\beta} - \vec{X}\right|$$
$$\overrightarrow{D_\delta} = \left|\overrightarrow{C_3} * \overrightarrow{X_\delta} - \vec{X}\right|$$

$\vec{D}_\alpha$, $\vec{D}_\beta$, and $\vec{D}_\delta$: modified detachment vector amid the α, β, and Δ-wolve location to the other wolves and $\vec{C}_1$, $\vec{C}_2$, and $\vec{C}_3$ represents constant vector used to adjust detachment vector (eq. 3). $\vec{X}$location of vector of other grey wolf (Ω).

$$\overrightarrow{X_1} = \overrightarrow{X_\alpha} - \overrightarrow{A_1} * \left(\overrightarrow{D_\alpha}\right),$$
$$\overrightarrow{X_2} = \overrightarrow{X_\beta} - \overrightarrow{A_2} * \left(\overrightarrow{D_\beta}\right),$$
$$\overrightarrow{X_3} = \overrightarrow{X_\delta} - \overrightarrow{A_3} * \left(\overrightarrow{D_\delta}\right),$$

where $\vec{X}_1$: new location vector obtained using α-wolves situation$\vec{X}_\alpha$, and $\vec{D}_\alpha$,$\vec{X}_2$: new location vector gained using β-wolves position $\vec{X}_\beta$and $\vec{D}_\beta$, $\vec{X}_3$: new position vector from Δ-wolves situation$\vec{X}_\delta$ and $\vec{D}_\beta$, and $\vec{A}_1$, $\vec{A}_2$, and $\vec{A}_3$; coefficient vectors (eq. 2).

$$\vec{A}(k+1) = \frac{\sum_{i=1}^{n} \overrightarrow{X_\iota}}{n},$$

where $\vec{X}(K+1)_1$ is new situation vector as average of all circumstances of α,β and Δ-wolves and n representing α,β and Δ-wolves (n = 3).

Attacking phase helps to classify local solutions. Local search performs variation in $\vec{A}_1$ in the interval [-2a to +2a]. If the value of constant vector $|A|$ < 1 then local search is achieved. With these machinists, search and update of situations performed to obtain optimal value. Search of prey phase is helping in deviating each other to find for prey and join to attack prey. If $|\vec{A}|$> 1 then search deviates from prey and bargains the new prey.

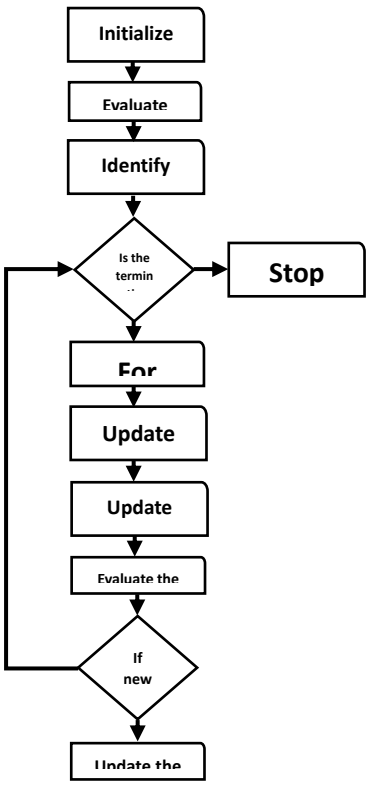

Figure 3. Flowchart of GWO algorithm

Table 1. Branch incidence matrix.

Branch	1	2	3	4	5
1	I	-I	N	N	-I
2	N	I	-I	-I	N
3	N	N	I	N	N
4	N	N	N	I	N
5	N	N	N	N	I

$$I_{br} = B^{-1} I_b$$

Using a B matrix, the link between branch currents and bus currents is brought about by the complex branch powers and bus powers. At the sending and receiving ends of the bus, the system's branch power losses Lbr produce different voltages. Similar to how bus/branch currents are established, so too is the relationship between branch powers and bus powers.

$$S_b = B[S_{br} - L_{br}]$$
$$S_{br} = B^{-1} S_b + L_{br}$$

S_{br}represents the apparent power of the branch. Sb is the perceived power of the bus. The matrix of bus incidence is B. We call the branch losses L_{br}. Complex quadratic equations make up the power flow equations. As in (4), a new variable called β_{lm} is established for a branch that connects the lth and mth buses.

$$\beta_{lm} = V_l(V_l^* - V_m^*)$$

where V_l is the lth bus voltage. V_l^* is the voltage conjugate solution of the lth bus. The branch control of the 'lm' th element is articulated in terms of β_{lm} as in (5).

$$S_{lm} = P_{lm} + jQ_{lm} = \beta_{lm} Y_{lm}^*$$
$$\beta_{lm} = S_{lm} Z_{lm}^*$$
$$V_m = V_l - \frac{\beta_{lm}^*}{V_l^*}$$
$$I_{lm} = \left(\frac{\beta_{lm}^*}{V_l^*}\right) Y_{lm}$$

The thorough flowchart is shown in figure 3`

$$S_{lm} = S_{ml} - L_{lm}$$
$$L_{lm} = \sum L_{lm}^r$$
$$L_{lm}^r = S_m^{spec_{r-1}} - V_m^{r-1} I_m^*$$
$$S_{br}^{rec} = S_{br}^{send} - L_{loss}$$
$$\text{Max}\,(L_{lm}^r) \le 0.01$$

Where

r is the repetition count.

L_{lm} is lm division losses.

S_m^{spec} is quantifiedseeming power at mth bus.

V_m is mth bus power.

I_m is mth bus present.

In light of the voltage stability restriction, the algorithm's constraints are being examined (Ramana, Ganesh, and Sivanagaraju 2010). When transmission losses are lower, the algorithm will operate more quickly in those systems. The transmission loss of each element in its rth iteration must be less than the tolerance value in order to meet the convergence requirements.[6]

Table 3 a: Test 1 Fitness value in each Iter under Attempt 2 Allocation of EVCS locations without DG

Iter 1 Fitness value:436.6502	Iter 19 Fitness value:436.6502	Iter 37 Fitness value:433.8815
Iter 2 Fitness value:436.6502	Iter 20 Fitness value:436.6502	Iter 38 Fitness value:433.8815
Iter 3 Fitness value:436.6502	Iter 21 Fitness value:436.6502	Iter 39 Fitness value:433.8815
Iter 4 Fitness value:436.6502	Iter 22 Fitness value:436.6502	Iter 40 Fitness value:433.8815
Iter 5 Fitness value:436.6502	Iter 23 Fitness value:436.6502	Iter 41 Fitness value:433.8815
Iter 6 Fitness value:436.6502	Iter 24 Fitness value:436.6502	Iter 42 Fitness value:433.8815
Iter 7 Fitness value:436.6502	Iter 25 Fitness value:436.6502	Iter 43 Fitness value:433.8815
Iter 8 Fitness value:436.6502	Iter 26 Fitness value:436.6502	Iter 44 Fitness value:433.8815
Iter 9 Fitness value:436.6502	Iter 27 Fitness value:433.8815	Iter 45 Fitness value:433.8815
Iter 10 Fitness value:436.6502	Iter 28 Fitness value:433.8815	Iter 46 Fitness value:433.8815
Iter 11 Fitness value:436.6502	Iter 29 Fitness value:433.8815	Iter 47 Fitness value:433.8815
Iter 12 Fitness value:436.6502	Iter 30 Fitness value:433.8815	Iter 48 Fitness value:433.8815
Iter 13 Fitness value:436.6502	Iter 31 Fitness value:433.8815	Iter 49 Fitness value:433.8815
Iter 14 Fitness value:436.6502	Iter 32 Fitness value:433.8815	Iter 50 Fitness value:433.8815
Iter 15 Fitness value:436.6502	Iter 33 Fitness value:433.8815	
Iter 16 Fitness value:436.6502	Iter 34 Fitness value:433.8815	
Iter 17 Fitness value:436.6502	Iter 35 Fitness value:433.8815	
Iter 18 Fitness value:436.6502	Iter 36 Fitness value:433.8815	

Table 3b: Information of EVCS used in this study

	EVCS (Bus)	Total Real Power(kW)	Total Reactive Power(kVAR)
EVCS 1	20	133.4	82.674
EVCS 2	3	249.52	154.64
EVCS 3	6	258.14	159.98
EVCS 4	7	375.7	232.84
EVCS 5	13	394.38	244.41

Table 3c: Voltage Profile of system Without DG (Voltage Deviation = VD)

EVCS Location					Minimum Voltage (pu)	VD (%)
2	3	6	7	13	0.86531	25.417

Table 3 d: Total Real and Reactive Power loss of system

Power-Loss (KW):	408.4649
Power-Loss (KVar):	275.1488

Table 5a: Test 1 Fitness value in each Iter under Allocation of EVCS locations with 1000 kw DG location

Iter 1 Fitness value:154.3212	Iter 19 Fitness value:133.5735	Iter 37 Fitness value:133.5735
Iter 2 Fitness value:146.9288	Iter 20 Fitness value:133.5735	Iter 38 Fitness value:133.5735
Iter 3 Fitness value:145.8589	Iter 21 Fitness value:133.5735	Iter 39 Fitness value:133.5735
Iter 4 Fitness value:142.5835	Iter 22 Fitness value:133.5735	Iter 40 Fitness value:133.5735
Iter 5 Fitness value:135.8673	Iter 23 Fitness value:133.5735	Iter 41 Fitness value:133.5735
Iter 6 Fitness value:135.8673	Iter 24 Fitness value:133.5735	Iter 42 Fitness value:133.5735
Iter 7 Fitness value:135.8673	Iter 25 Fitness value:133.5735	Iter 43 Fitness value:133.5735
Iter 8 Fitness value:134.1778	Iter 26 Fitness value:133.5735	Iter 44 Fitness value:133.5735
Iter 9 Fitness value:133.5735	Iter 27 Fitness value:133.5735	Iter 45 Fitness value:133.5735
Iter 10 Fitness value:133.5735	Iter 28 Fitness value:133.5735	Iter 46 Fitness value:133.5735
Iter 11 Fitness value:133.5735	Iter 29 Fitness value:133.5735	Iter 47 Fitness value:133.5735
Iter 12 Fitness value:133.5735	Iter 30 Fitness value:133.5735	Iter 48 Fitness value:133.5735
Iter 13 Fitness value:133.5735	Iter 31 Fitness value:133.5735	Iter 49 Fitness value:133.5735
Iter 14 Fitness value:133.5735	Iter 32 Fitness value:133.5735	Iter 50 Fitness value:133.5735
Iter 15 Fitness value:133.5735	Iter 33 Fitness value:133.5735	
Iter 16 Fitness value:133.5735	Iter 34 Fitness value:133.5735	

Table 5 b: Information of EVCS used in this study

	EVCS (Bus)	Total Real Power(kW)	Total Reactive Power(kVAR)
EVCS 1	21	133.4	82.674
EVCS 2	23	249.52	154.64
EVCS 3	26	258.14	159.98
EVCS 4	8	375.7	232.84
EVCS 5	15	394.38	244.41

Table 5 c: Power loss of system with DG location (COMPARED TO NO DG)

DG Location					P Loss Reduction (kw)	P Loss Reduction (%)
5	32	16			280.87	68.766

Table 5 d: Voltage Profile of system with DG size and location (Voltage Deviation = VD) (COMPARED TO NO DG)

DG Location			Minimum Voltage	VD (%)	VD Reduction (%)	VD Improvement
5	32	16	0.94239	5.9994	19.461	76.436

Table 5 e: Total Real and Reactive Power loss of system

Power-Loss (KW):	127.574
Power-Loss(KVar):	87.9325

Table 4 a: Test 1 Fitness value in each Iter under Attempt 3 Allocation of EVCS locations without DG

Iter 1 Fitness value:452.825	Iter 19 Fitness value:432.4796	Iter 37 Fitness value:432.4796
Iter 2 Fitness value:452.825	Iter 20 Fitness value:432.4796	Iter 38 Fitness value:432.4796
Iter 3 Fitness value:432.4796	Iter 21 Fitness value:432.4796	Iter 39 Fitness value:432.4796
Iter 4 Fitness value:432.4796	Iter 22 Fitness value:432.4796	Iter 40 Fitness value:432.4796
Iter 5 Fitness value:432.4796	Iter 23 Fitness value:432.4796	Iter 41 Fitness value:432.4796
Iter 6 Fitness value:432.4796	Iter 24 Fitness value:432.4796	Iter 42 Fitness value:432.4796
Iter 7 Fitness value:432.4796	Iter 25 Fitness value:432.4796	Iter 43 Fitness value:432.4796
Iter 8 Fitness value:432.4796	Iter 26 Fitness value:432.4796	Iter 44 Fitness value:432.4796
Iter 9 Fitness value:432.4796	Iter 27 Fitness value:432.4796	Iter 45 Fitness value:432.4796
Iter 10 Fitness value:432.4796	Iter 28 Fitness value:432.4796	Iter 46 Fitness value:432.4796
Iter 11 Fitness value:432.4796	Iter 29 Fitness value:432.4796	Iter 47 Fitness value:432.4796
Iter 12 Fitness value:432.4796	Iter 30 Fitness value:432.4796	Iter 48 Fitness value:432.4796
Iter 13 Fitness value:432.4796	Iter 31 Fitness value:432.4796	Iter 49 Fitness value:432.4796
Iter 14 Fitness value:432.4796	Iter 32 Fitness value:432.4796	Iter 50 Fitness value:432.4796
Iter 15 Fitness value:432.4796	Iter 33 Fitness value:432.4796	
Iter 16 Fitness value:432.4796	Iter 34 Fitness value:432.4796	
Iter 17 Fitness value:432.4796	Iter 35 Fitness value:432.4796	
Iter 18 Fitness value:432.4796	Iter 36 Fitness value:432.4796	

Table 4b: Information of EVCS used in this study

	EVCS (Bus)	Total Real Power(kW)	Total Reactive Power (kVAR)
EVCS 1	2	133.4	82.674
EVCS 2	4	249.52	154.64
EVCS 3	6	258.14	159.98
EVCS 4	7	375.7	232.84
EVCS 5	13	394.38	244.41

Table 4c: Voltage Profile of system Without DG (Voltage Deviation = VD)

EVCS Location					Minimum Voltage (pu)	VD (%)
2	4	6	7	13	0.86531	25.401

Table 4 d: Total Real and Reactive Power loss of system

Power-Loss (KW):	407.0787
Power-Loss (KVar):	273.8875

Table2a: Test 1 Fitness value in each iteration under Attempt 1 Allocation of EVCS locations without DG

Iter 1 Fitness value:446.8525	Iter 19 Fitness value:440.0878	Iteration 37 Fitness value:440.0878
Iter 2 Fitness value:446.8525	Iter 20 Fitness value:440.0878	Iter 38 Fitness value:440.0878
Iter 3 Fitness value:444.5651	Iter 21 Fitness value:440.0878	Iter 39 Fitness value:440.0878
Iter 4 Fitness value:440.0878	Iter 22 Fitness value:440.0878	Iter 40 Fitness value:440.0878
Iter 5 Fitness value:440.0878	Iter 23 Fitness value:440.0878	Iter 41 Fitness value:440.0878
Iter 6 Fitness value:440.0878	Iter 24 Fitness value:440.0878	Iter 42 Fitness value:440.0878
Iter 7 Fitness value:440.0878	Iter 25 Fitness value:440.0878	Iter 43 Fitness value:440.0878
Iter 8 Fitness value:440.0878	Iter 26 Fitness value:440.0878	Iter 44 Fitness value:440.0878
Iter 9 Fitness value:440.0878	Iter 27 Fitness value:440.0878	Iter 45 Fitness value:440.0878
Iter 10 Fitness value:440.0878	Iter 28 Fitness value:440.0878	Iter 46 Fitness value:440.0878
Iter 11 Fitness value:440.0878	Iter 29 Fitness value:440.0878	Iter 47 Fitness value:440.0878
Iter 12 Fitness value:440.0878	Iter 30 Fitness value:440.0878	Iter 48 Fitness value:440.0878
Iter 13 Fitness value:440.0878	Iter 31 Fitness value:440.0878	Iter 49 Fitness value:440.0878
Iter 14 Fitness value:440.0878	Iter 32 Fitness value:440.0878	Iter 50 Fitness value:440.0878
Iter 15 Fitness value:440.0878	Iter 33 Fitness value:440.0878	
Iter 16 Fitness value:440.0878	Iter 34 Fitness value:440.0878	
Iter 17 Fitness value:440.0878	Iter 35 Fitness value:440.0878	
Iter 18 Fitness value:440.0878	Iter 36 Fitness value:440.0878	

Table 2b: Information of EVCS used in this study

	EVCS (Bus)	Total Real Power(kW)	Total Reactive Power(kVAR)
EVCS 1	2	133.4	82.674
EVCS 2	4	249.52	154.64
EVCS 3	6	258.14	159.98
EVCS 4	7	375.7	232.84
EVCS 5	13	394.38	244.41

Table 2 c: Voltage Profile of system Without DG (Voltage Deviation = VD)

EVCS Location					Minimum Voltage (pu)	VD (%)
2	4	6	7	13	0.86439	25.818

Table 2 d: Total Real and Reactive Power loss of system

Power-Loss (KW):	414.2693
Power-Loss (KVar):	277.6772

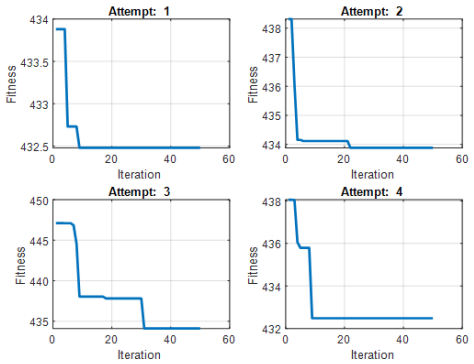

4. Conclusions

The emergence of fast charging technology has introduced additional challenges for the distribution system and EV charging infrastructure. While fast charging improves user convenience by significantly reducing charging times, it also imposes greater strains on the grid and charging stations. Careful planning and management are essential to mitigate the possible adverse effects of fast accusing on the circulation system and charging infrastructure.

In recent years, there has been a surge in studies focusing on optimal EV charging station locations and the impacts of EV demand on the circulation network. Researchers have explored various strategies for deploying EV charging stations, aiming to minimize voltage deviations, enhance system reliability, and reduce overall power losses. Additionally, studies have investigated different investment models for deploying EV charging infrastructure. However, there has been limited attention given to understanding the preferences and behaviors of EV users when selecting charging station locations.

In summary, the work mentioned here appears to provide a comprehensive overview of the various aspects involved in optimizing charging station locations, including problem formulation, solution techniques, and considerations such as EV load modeling, uncertainty handling, renewable energy integration, and V2G strategies. Metaheuristic algorithms are highlighted as effective tools for achieving better optimization results in this context. Understanding the preferences and behaviors of EV users is crucial for effective planning and deployment of charging infrastructure as a future scope. By considering factors such as travel patterns, charging habits, and user preferences, planners can optimize the placement of charging positions to better meet the needs of EV users while minimizing the impact on the distribution network. This holistic approach will be essential for ensuring the successful addition of EVs into the

conveyance system while maintaining grid stability and reliability.

Reference

[1] Brockway, P. E., Owen, A., Brand-Correa, L. I., and Hardt, L. (2019). Estimation of Global Final-Stage Energy-Return-On-Investment for Fossil Fuels with Comparison to Renewable Energy Sources. Nat. Energ. 4 (7), 612–621. doi:10.1038/s41560-019-0425-z

[2] Dong, L., Li, J., Pu, T., and Chen, N. (2019). Distributionally Robust Optimization Model of Active Distribution Network Considering Uncertainties of Source and Load. J. Mod. Power Syst. Clean. Energ. 7 (6), 1585–1595. doi:10.1007/s40565- 019-0558-x

[3] Elbatawy, S., and Morsi, W. (2022). Integration of Prosumers with Battery Storage and Electric Vehicles via Transactive Energy. IEEE Trans. Power Deliv. 37 (1), 383–394. doi:10.1109/tpwrd.2021.3060922

[4] Fang, B., Li, B., Li, X., Jia, Y., Xu, W., and Liao, Y. (2021). Multi-Objective Comprehensive Charging/Discharging Scheduling Strategy for Electric Vehicles Based on the Improved Particle Swarm Optimization Algorithm. Front. Energ. Res. 9, 811964. doi:10.3389/fenrg.2021.811964

[5] Islam, M. R., Lu, H., Hossain, J., Islam, M. R., and Li, L. (2020). Multiobjective Optimization Technique for Mitigating Unbalance and Improving Voltage Considering Higher Penetration of Electric Vehicles and Distributed Generation. IEEE Syst. J. 14 (3), 3676–3686. doi:10.1109/jsyst.2020.2967752

[6] Jiao, F., Zou, Y., and Zhang, X. (2021). A Three-Stage Multi-Timescale Framework for Online Dispatch in a Microgrid with EVs and Renewable Energy [J]. IEEE Trans. Trans Electri. 1 1. doi:10.1109/tte.2021.3098687

[7] Luo, Y., Feng, G., Wan, S., Zhang, S., Li, V., and Kong, W. (2020). Charging Scheduling Strategy for Different Electric Vehicles with Optimization for Convenience of Drivers, Performance of Transport System and Distribution Network. Energy 194, 116807. doi:10.1016/j.energy.2019.116807

[8] Mahmoudi, S. K., Golshan, M. E. H., and Zamani, R. (2021). Coordinated Voltage Control Scheme for Transmission System Considering Objectives and Constraints of Network and Control Devices. Electric Power Syst. Res. 192, 106908. doi:10.1016/j.epsr.2020.106908

[9] Peidong, Z., Yanli, Y., jin, S., Yonghong, Z., Lisheng, W., and Xinrong, L. (2009). Opportunities and Challenges for Renewable Energy Policy in China. Renew. Sust. Energ. Rev. 13 (2), 439–449. doi:10.1016/j.rser.2007.11.005

[10] Battapothula, G., Yammani, C., Maheswarapu, S., 2019a. Multi-objective optimal planning of FCSs and DGs in distribution system with future EV load enhancement. IET Electr. Syst. Transp. 9 (3), 128–139.

[11] Tian, Y.-f., Liao, R.-j., Farkoush, S.G., 2021. Placement and sizing of EESS bundled with uncertainty modeling by two-stage stochastic search based on improved shark smell optimization algorithm in micro-grids. Energy Rep. 7, 4792–4808.

[12] Zhu, Z.-h., Gao, Z.-y., Zheng, J.-f., Du, H.-m., 2016. Charging station location problem of plug-in electric vehicles. J. Transp. Geogr. 52, 11–22.

[13] Luo, X., Qiu, R., 2020. Electric vehicle charging station location towards sustainable cities. Int. J. Environ. Res. Public Health 17 (8).

[14] Xiang, Y., Liu, J., Li, R., Li, F., Gu, C., Tang, S., 2016. Economic planning of electric vehicle charging stations considering traffic constraints and load profile templates. Appl. Energy 178, 647–659.

[15] Sadeghi-Barzani, P., Rajabi-Ghahnavieh, A., Kazemi-Karegar, H., 2014. Optimal fast charging station placing and sizing. Appl. Energy 125, 289–299.